2018 IEEE EMBS International Conference on Biomedical & Health Informatics (BHI)
4-7 March 2018
Las Vegas, Nevada, USA

Deep EEG Super-resolution: Upsampling EEG Spatial Resolution with Generative Adversarial Networks

Isaac A. Corley, *Member, IEEE*, Yufei Huang, *Senior Member, IEEE*

***Abstract*— Electroencephalography (EEG) activity contains a wealth of information about what is happening within the human brain. Recording more of this data has the potential to unlock endless future applications. However, the cost of EEG hardware is increasingly expensive based upon the number of EEG channels being recorded simultaneously. We combat this problem in this paper by proposing a novel deep EEG super-resolution (SR) approach based on Generative Adversarial Networks (GANs). This approach can produce high spatial resolution EEG data from low resolution samples, by generating channel-wise upsampled data to effectively interpolate numerous missing channels, thus reducing the need for expensive EEG equipment. We tested the performance using an EEG dataset from a mental imagery task. Our proposed GAN model provided ~10^4 fold and ~10^2 fold reduction in mean-squared error (MSE) and mean-absolute error (MAE), respectively, over the baseline bicubic interpolation method. We further validate our method by training a classifier on the original classification task, which displayed minimal loss in accuracy while using the super-resolved data. The proposed SR EEG by GAN is a promising approach to improve the spatial resolution of low density EEG headset.**

I. INTRODUCTION

Electroencephalography (EEG) is a noninvasive neuroimaging modality widely used for clinical diagnosis of seizures and cognitive neuroscience. It has gained increasing popularity in recent years as a neurofeedback device in brain-computer interface (BCI) systems with applications including typing interface for locked-in patients, neurorehabilitation [1], brain-controlled drone [2], and detection of driver fatigue [3]. However, a primary bottleneck to EEG-based BCI research is the cost of hardware. Ideally, EEG devices with high density channels are preferred in order to obtain recordings of brain activities with high spatial resolution underlying different cognitive events. However, the cost of EEG hardware increases exponentially with channels, with a majority of commercial EEG devices with 32 channels costing more than $20k. For academia and industry, this can greatly hinder the quality of products and research being performed. This also results in poor generality for EEG-based algorithms because prediction algorithms developed using one headset cannot be used for a headset of different channels even if both are used to measure the same cognitive events. EEG channel interpolation has been proposed in many research efforts [4][5] to recreate missing or defective sensor channels. Although they showed favorable improvement for single selective channel interpolation, research for interpolating many channels at a global scale is scarce.

Deep learning and its applications have recently become highly popular and rightly so, due to their superior ability to learn representations of complex data [6]. One of its applications is image super-resolution (SR), where deep learning based pixel interpolation was developed [7] to generate high resolution (HR) copies from low resolution (LR) images. The state-of-the-art SR performance is obtained by the new game theoretic deep generative model of Generative Adversarial Networks (GANs) [8], which established the first framework to achieve photo-realistic natural images for a 4x upscaling factor [9].

Inspired by the similarity between global EEG channel interpolation and image SR along with the superb image SR performance achieved by GANs, we propose deep EEG super-resolution, a novel framework for generating high spatial resolution EEG data from low resolution recordings using GANs. We compare our work to a baseline of bicubic interpolation and then additionally verify performance through training a classifier using the SR EEG data for the original EEG dataset's classification purpose.

II. DATA

A. Berlin BCI Competition III, Dataset V

Dataset V of the Berlin Brain Computer Interface Competition III provided by the IDIAP Research Institute [10] was used The dataset consists of 32 EEG channels recorded at 512 Hz for 3 individual subjects, located at the standard positions of the International 10-20 system (Fp1, AF3, F7, F3, FC1, FC5, T7, C3, CP1, CP5, P7, P3, Pz, PO3, O1, Oz, O2, PO4, P4, P8, CP6, CP2, C4, T8, FC6, FC2, F4, F8, AF4, Fp2, Fz, Cz). The dataset was initially used for a mental imagery multiclass classification competition of three labeled tasks. The data is provided with train and test sets for each subject; however, only the train set was used due to the test set not being provided with labels. The train set contained a total of 1,096,192 samples.

B. Preprocessing

Following the epoch extraction procedure in [10], the raw data was separated into epochs of length 512 samples using a moving window with a stride of 32 samples. This resulted in epochs of size (32 channels by 512 samples). The epoched data was then split into train, validation, and test sets for holdout validation using a 75/20/5 percentage split criterion.

The initial Dataset V classifiers used precomputed features, which consisted of the estimated power spectral

I. A. Corley is an Engineer at Southwest Research Institute (SwRI) and a graduate student of Electrical Engineering at the University of Texas at San Antonio, San Antonio, TX 78249 USA (e-mail: icorley@swri.org).

Y. Huang is with the Department of Electrical and Computer Engineering, University of Texas at San Antonio, San Antonio, TX 78249 USA (e-mail: yufei.huang@utsa.edu).

978-1-5386-2405-0/18/$31.00 ©2018 IEEE

density (PSD) of each epoch in the band 8-30 Hz with a frequency resolution of 2 Hz for the 8 centro-parietal channels (C3, Cz, C4, CP1, CP2, P3, Pz, P4), which resulted in a 96-dimensional vector (8 channels, 12 frequency components).

For use with super-resolution models, all datasets were reshaped to epochs of size (32 channels by 64 samples). To produce the low-resolution (LR) data, the epochs were downsampled by channel based upon the scale factor used, e.g., downsampling 32 channels by a scale factor of 2 would remove every other channel, leaving 16 channels of LR data. The removed channels are then used as the HR data. The input data and its corresponding ground truth were then standard-normalized to a mean $\mu = 0$ and standard deviation $\sigma = 1$ using the mean and standard deviation of the input channel training set. This was repeated using the same statistics for normalizing the validation and test data.

III. METHODS

A. Generative Adversarial Networks

Generative Adversarial Networks (GANs) are an unsupervised deep learning framework recently proposed by Goodfellow et al. [8]. The framework is composed of two networks, a generator *G* and a discriminator *D*, optimized to minimize a two-player minimax game, where the generator learns to fool the discriminator and the discriminator learns to prevent itself from being fooled. As Goodfellow et al. [8] describes, "*The generative model can be thought of as analogous to a team of counterfeiters, trying to produce fake currency and use it without detection, while the discriminative model is analogous to the police, trying to detect the counterfeit currency.*" During training of GANs, the generator is fed an input noise vector and produces an output distribution P_G. The discriminator is then trained to learn to discriminate between P_G and the true data distribution, P_{Data}. Additionally, the generator is trained to learn how to further fool the discriminator. Theoretically P_G will converge to P_{Data} with the discriminator being unable to differentiate between generated and true samples, resulting in an ideal generative model which can produce data following the true data distribution.

While GANs are a powerful framework, they possess stability issues which cause the adversarial networks to rarely reach convergence. Variations of the framework, namely Wasserstein GANs (WGANs) [11][12], have been developed which use different loss functions with properties that improve training stability. In contrast to the original GAN framework, WGANs minimize the Earth Mover's Distance (Wasserstein-1 Distance) and attempt to constrain the gradient norm of the discriminator's output with respect to its input using a gradient penalty in the loss function. We adopt the WGAN framework for training throughout our research as we experienced improved stability over the original GAN framework.

B. Proposed Wasserstein Generative Adversarial Networks for EEG Super Resolution

Our proposed WGAN model for EEG SR also consists of a generator and a discriminator. The generator architecture consists of the sequence of layers detailed in Figure 1. with the parameters detailed in TABLE I. Similarly to [11] we adopt a modified sequence of convolutional layers, which allow EEG data to be processed by Convolutional Neural Networks (CNNs) due to correlations across channels. This sequence is composed of convolutional layers with kernel dimensions that find the relationships between channels, (n, 1), where n = (# input channels + 1). All convolutional layers enforce the same zero-padding to keep the same dimensions throughout. This sequence is then fed into one dense block [14] composed of 3 densely connected convolutional sequences, followed by a convolutional layer whose outputs are the super resolved channels. Note that the upsampling layer and the first subsequent convolutional layer are unique to SR models for a scale factor of 4 as the input channels need to be upsampled by 3 channel-wise.

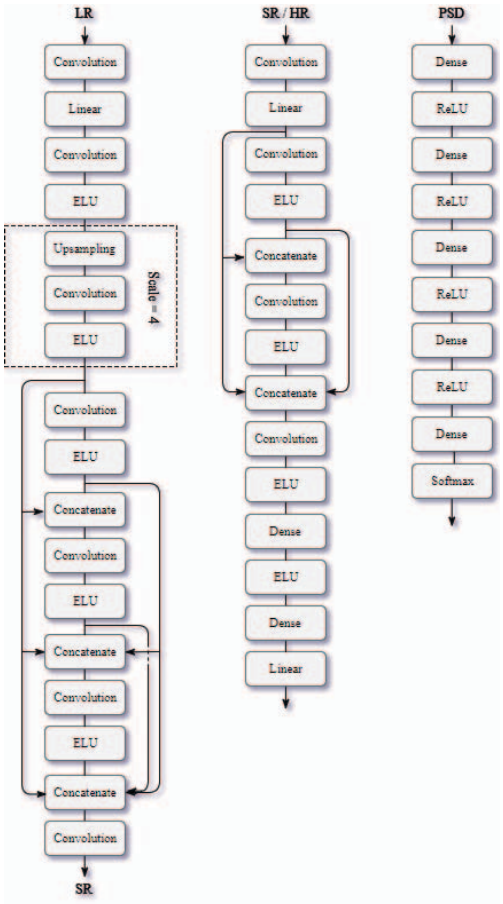

Figure 1. Model Architectures. *Generator (left), Discriminator (center), Classifier (right)*

TABLE I. GENERATOR MODEL ARCHITECTURE

Layer Type	Kernels	Dimensions	Activation
Convolution	128	(# input channels + 1, 1)	Linear
Convolution	128	(# input channels / 2 + 1, 1)	ELU
Upsampling	-	(scale factor – 1, 1)	-
Convolution	128	(# input channels + 1, 1)	ELU
Convolution	128	(# input channels / 2 + 1, 1)	ELU

Layer Type	Kernels	Dimensions	Activation
Concatenate	-	-	-
Convolution	256	(# input channels / 2 + 1, 1)	ELU
Concatenate	-	-	-
Convolution	512	(# input channels / 2 + 1, 3)	ELU
Concatenate	-	-	-
Convolution	1	(# input channels + 1, 1)	None

The discriminator follows a similar scheme to the generator architecture aside from a few key differences detailed in TABLE II. The 4th convolutional layer has a stride of (4, 4) and is fed into a fully-connected layer. The final output activation of the model is linear to comply with the WGAN framework.

As in [9], the generator's parameters are first initialized through training the network in a supervised manner to map the downsampled LR data to the HR counterparts using a mean-squared error (MSE) loss function. This was found to prevent converging to local minima. The generator is then inserted into the GAN training process to fine-tune the model and find more optimal parameters in comparison to only using a distance metric as a loss function.

TABLE II. DISCRIMINATOR MODEL ARCHITECTURE

Layer Type	Kernels	Dimensions	Activation
Convolution	64	(# input channels + 1, 1)	Linear
Convolution	64	(1, 3)	ELU
Concatenate	-	-	-
Convolution	128	(# input channels / 2 + 1, 1)	ELU
Concatenate	-	-	-
Convolution	256	(# input channels / 4 + 1, 3)	ELU
Fully-Connected	128	-	ELU
Fully-Connected	1	-	Linear

IV. RESULTS

A. Training & Hyperparameters

Dropout regularization [15] was applied at the output of every activation within both the generator and discriminator excluding the output layers. The generator and discriminator had dropout rates of 0.1 and 0.25, respectively. The α parameter for all ELU [16] activations was set to 1. The Adam optimizer [17] was used throughout with learning rate $\alpha = 10^{-4}$, $\beta_1 = 0.5$, and $\beta_2 = 0.9$. The generator network was first pre-trained using a MSE (L2) loss for 50 epochs with a mini-batch size of 64. All hyperparameters were tuned to optimize performance on the validation set.

The pre-trained generator was then fine-tuned using the WGAN framework losses using a gradient penalty weight of 10. The GAN training ratio was set to 3, which updates the discriminator once for every 3 generator updates. In addition to the WGAN loss function, a modification was made to multiply the WGAN loss by a factor of 10^{-2} and add a MSE loss on the generator output. This was inspired by the feature matching procedure from [18], which specifies additional objectives for the generator to prevent from overtraining on the discriminator. Also from [18], the label smoothing technique was incorporated, to assist in avoiding converging to local minima.

An evaluation of the model outputs of the validation and test datasets are displayed in TABLE III. The quantitative results are compared to a baseline of bicubic interpolated channel data. Both MSE and mean absolute error (MAE) between upsampled and true EEG signals were calculated.

TABLE III. SUPER RESOLUTION PERFORMANCE RESULTS

Dataset	Scale	Bicubic		WGAN	
		MSE	MAE	MSE	MAE
Val	2	3.71E7	3.89E3	**2.01E3**	**24.38**
	4	7.23E7	6.42E3	**8.53E3**	**63.83**
Test	2	3.75E7	3.91E3	**2.06E3**	**24.66**
	4	7.30E7	6.45E3	**8.68E3**	**64.39**

B. Dataset V Classification Super Resolution Performance

To further evaluate the validity of the SR data, we investigated the performance of classifying the mental imagery classes using the SR data. Deep neural network (DNN) classifiers were trained for both the precomputed features of the HR and SR data using the precomputed feature class labels. The DNN classifier consisted of 5 dense layers with 512, 256, 128, 64, and 3 neurons per layer, respectively. All layers contained ReLU [19] activations excluding the output layer which consisted of a Softmax activation. The classifiers were trained using a categorical cross-entropy loss optimized by the ADAM optimizer with learning rate $\alpha = 10^{-3}$, $\beta_1 = 0.9$, and $\beta_2 = 0.99$. The class predictions with multiple metrics for the DNNs trained using the ground truth HR data and SR data by WGAN are recorded in TABLE IV.

TABLE IV. CLASSIFICATION PERFORMANCE RESULTS

Scale	Metric (%)	Class	HR		WGAN	
			Val	Test	Val	Test
2	Accuracy	-	89.56	87.75	85.63	83.88
	Precision	2	89.70	86.65	83.98	82.24
		3	89.48	87.54	85.80	82.84
		7	89.57	88.77	86.80	86.12
	Recall	2	87.66	84.33	83.86	80.21
		3	88.49	88.57	83.84	84.37
		7	92.06	89.62	88.69	86.26
4	Accuracy	-	89.56	87.75	81.31	82.00
	Precision	2	89.70	86.65	79.55	80.21
		3	89.48	87.54	81.21	82.03
		7	89.57	88.77	82.79	83.28
	Recall	2	87.66	84.33	78.13	77.73
		3	88.49	88.57	82.21	81.34
		7	92.06	89.62	83.05	85.94

V. Discussion

On the topic of CNNs for EEG time-series data, we highlight below some of the important findings throughout our research. Feature scaling techniques besides standard normalization decreased model performance. With regards to convolutional layers, using kernel dimensions that contained weights for each channel in the input and output layers improved performance significantly over the standard kernel dimensions used for images, e.g., 3x3, 9x9. Implementing concatenation connections instead of residual connections, popular in ResNet [20] architectures used in many Super Resolution papers, offered improved performance using a lesser amount of layers. A Linear activation on the input layer followed by ELU activations on the subsequent layers outperformed other popular neural network activation functions combinations.

It was notably difficult and time-consuming to train GANs for EEG data. We observed after testing different variants of GAN that WGAN appeared to be more stable during training. Replacing MSE with MAE in all loss functions produced SR EEG signals which were smoothed and did not contain similar frequency domain statistics as the HR data. It can be concluded the task of EEG SR is highly sensitive to the loss function components used during training.

Observing the results in TABLE III. compared to bicubic interpolation, WGAN achieved $\sim 10^4$ fold and $\sim 10^2$ fold reduction in MSE and MAE, respectively, demonstrating the remarkable improvement of our proposed WGAN method in simultaneously reconstructing numerous missing EEG signals at a high resolution. Judging from the results in TABLE IV. it can be observed that classification of SR data produces minimal loss of accuracy when compared to ground truth signals, less than 4% and 9% for scale factors of 2 and 4, respectively.

VI. Conclusion

Our results conclude that our WGAN methods significantly improved over bicubic interpolation for the Dataset V EEG signals. We conclude that SR EEG by GAN is a promising approach to improve the spatial resolution of low density EEG headset. However we intend to expand our work to perform well across multiple datasets for different classification tasks. Considerations for further work also include using different distance metrics than MSE for assessing signal similarity as well as using other recent variations of the GAN framework to compare results.

Acknowledgment

This work was supported by the Army Research Laboratory Cognition and Neuroergonomics Collaborative Technology Alliance (CANCTA) under Cooperative Agreement Number W911NF-10-2-0022.

References

[1] J. Wolpaw and D. McFarland, "Multichannel EEG-based brain-computer communication," *Electroencephalography and Clinical Neurophysiology*, vol. 90, pp. 444-449, 1994.

[2] L. Meriño, T. Nayak, P. Kolar, G. Hall, Z. Mao, D. J. Pack, and Y. Huang, "Asynchronous control of unmanned aerial vehicles using a steady-state visual evoked potential-based brain computer interface," *Brain-Computer Interfaces*, vol. 4, pp., 122-135, 2017

[3] M. Hajinoroozi, Z. Mao, T-P Jung, C-T Lin, and Y. Huang "EEG-based Prediction of Driver's Cognitive Performance by Deep Convolutional Neural Network," *Signal Processing: Image Communication,* vol. 47, pp. 549-555, 2016.

[4] S. Petrichella *et al*., "Channel interpolation in TMS-EEG: A quantitative study towards an accurate topographical representation," *2016 38th Annual International Conference of the IEEE Engineering in Medicine and Biology Society (EMBC)*, pp. 989-992, 2016

[5] H. S. Courellis, J. R. Iversen, H. Poizner and G. Cauwenberghs, "EEG channel interpolation using ellipsoid geodesic length," *2016 IEEE Biomedical Circuits and Systems Conference (BioCAS)*, Shanghai, 2016, pp. 540-543. doi: 10.1109/BioCAS.2016.7833851

[6] Y. Lecun, Y. Bengio, and G. Hinton, "Deep learning," *Nature*, vol. 521, pp. 436-444, 2015. doi:10.1038/nature14539

[7] C. Dong, K. He, C. Loy, and X. Tang, "Image Super-Resolution Using Deep Convolutional Networks," *IEEE Transactions on Pattern Analysis and Machine Intelligence*, vol. 38, pp. 295-307, 2016.

[8] I. Goodfellow, J. Pouget-Abadie, M. Mirza, B. Xu, D. Warde-Farley, S. Ozair, A. Courville, and Y. Bengio, "Generative Adversarial Nets," *Advances in Neural Information Processing Systems*, vol. 27, pp. 2672-2680, 2014.

[9] C. Ledig, L. Theis, F. Huszar, J. Caballero, A. Aitken, A. Tejani, J. Totz, Z. Wang, and W. Shi, "Photo-Realistic Single Image Super-Resolution Using a Generative Adversarial Network", 2016.

[10] J. Millan, "On the need for on-line learning in brain-computer interfaces," *2004 IEEE International Joint Conference on Neural Networks* (IEEE Cat. No.04CH37541), 2004, pp. 2877-2882 vol.4. doi: 10.1109/IJCNN.2004.1381116

[11] M. Arjovsky, L. Bottou, and S. Chintala, "Wasserstein GAN," 2017.

[12] F. Ahmed, M. Arjovsky, A. Courville, V. Dumoulin, and I. Gulrajani, "Improved Training of Wasserstein GANs," 2017.

[13] W. Burgard, T. Ball, K. Eggensperger, L. Fiederer, M. Glasstetter, F. Hutter, R. Schirrmeister, J. Springenberg, and M. Tangermann, "Deep learning with convolutional neural networks for EEG decoding and visualization," Human brain mapping, vol. 38, pp. 5391-5420y 2017.

[14] G. Huang, Z. Liu, L. van der Maaten, and K. Weinberger, "Densely connected convolutional networks," in *Proceedings of the IEEE Conference on Computer Vision and Pattern Recognition*, 2017

[15] N. Srivastava, G. Hinton, A. Krizhevsky, I. Sutskever, and R. Salakhutdinov, "Dropout: A Simple Way to Prevent Neural Networks from Overfitting," *Journal of Machine Learning Research*, vol. 15, pp. 1929-1958, 2014.

[16] D. Clevert, T. Unterthiner, and S. Hochreiter, "Fast and Accurate Deep Network Learning by Exponential Linear Units (ELUs)," in *International Conference on Learning Representations*, 2016.

[17] D. P. Kingma and J. Lei Ba, "ADAM: A Method for Stochastic Optimization," in *International Conference on Learning Representations*, 2015.

[18] T. Salimans, I. Goodfellow, W. Zaremba, V. Cheung, A. Radford, X. Chen, "Improved Techniques for Training GANs," *Advances in Neural Information Processing Systems*, vol. 29, pp. 2234-2242, 2016.

[19] G. Hinton, and V. Nair, "Rectified Linear Units Improve Restricted Boltzmann Machines," *International Conference on Machine Learning*, 2010

[20] K. He, S. Ren, J. Sun, and X. Zhang, "Deep Residual Learning for Image Recognition," *IEEE Conference on Computer Vision and Pattern Recognition*, pp. 770-778, 2016